J. Cent. South Univ. (2018) 25: 2182−2189
DOI: https://doi.org/10.1007/s11771-018-3906-5

Springer

Direct fabrication of highly porous graphene/TiO_2 composite nanofibers by electrospinning for photocatalytic application

HE Yuan(何缘), LIU Yun-guo(刘云国)

College of Environmental Science and Engineering, Key Laboratory of Environmental Biology and Pollution, Hunan University, Changsha 410072, China

Abstract: We reported the fabrication of highly porous graphene/TiO_2 composite nanofibers in the form of a nonwoven mat by electrospinning followed by calcination in air at 450 °C. The graphene can uniformly disperse in highly porous TiO_2 nanofibers. The highly porous graphene/TiO_2 composite nanofibers exhibited excellent catalytic activities. The new method for producing graphene/TiO_2 composite nanofibers is versatile and can be extended to fabricate various types of metal oxide and graphene nanocomposites.

Key words: porous structure; graphene; titanium dioxide; photocatalytic application

Cite this article as: HE Yuan, LIU Yun-guo. Direct fabrication of highly porous graphene/TiO_2 composite nanofibers by electrospinning for photocatalytic application [J]. Journal of Central South University, 2018, 25(9): 2182–2189. DOI: https://doi.org/10.1007/s11771-018-3906-5.

1 Introduction

Nanomaterials are expected to play an increasingly important role in industrial manufacture due to their fascinating electronic and optoelectronic properties compared to their bulk counterparts [1–3]. Graphene, a perfect two-dimensional material, has become a new star on the horizon of nanomaterials since it was found in 2004 due to the extraordinary electronic properties, such as ballistic transport over 0.4 mm in length, quantum hall effect at room temperature, high electron mobility, and single-molecule field-effect sensitivity [4–8]. Graphene and its composites can be widely applied in many fields including photocatalysis, liquid crystal displays, lithium ion batteries, solar cells, wound healing [9], and so on [10–15]. So, fabrication of graphene composites is very interesting and important, especially for simple method to obtain graphene composites.

TiO_2 is regarded as one of the most important metal-oxide-semiconductors and has been found its applications in a wide range of fields, such as solar cells, photocatalysis, lithium-ion batteries, H_2 energy production, and antimicrobial activities [16–19]. However, the photoefficiency of TiO_2 is substantially limited by its large band gap energy (3.0–3.2 eV). It is very important for patenting environment remediation to developing visible-light-driven photocatalysts [20, 21]. The TiO_2 and graphene composites are currently being considered a potential material to develop visible-light-driven photocatalysts and improve the photoefficiency of TiO_2 [22]. So far, TiO_2/graphene composites (TGCs) have been fabricated by many kinds of methods, including molecular grafting, solvothermal method, and so on [23, 24]. However, most of the graphene/TiO_2 composites have been fabricated with complicated processes, and most of TiO_2 is

Foundation item: Project(41271332) supported by the National Natural Science Foundation of China
Received date: 2017−02−11; **Accepted date:** 2017−04−01
Corresponding author: LIU Yun-guo, PhD, Professor; Tel: +86−13974881035; E-mail: liuyunguo@hnu.edu.cn

of nanoparticles but not 1D nanostructures, which is more promising in the photocatalysis applications due to excellent mobility of charge carriers, scattering more light at the red part of the solar spectrum, and the existence of straight pores can enhance the accessibility of electrodes to the hole transporting materials and hence enhance charge collection and transport compared to nanoparticles in photovoltaic and photocatalysis applications [25, 26]. Thus it is desirable to develop a simple method to integrate graphene into one-dimensional (1D) nanostructured TiO_2 for enhanced photovoltaic and photocatalytic applications.

As a straightforward method to produce 1D nanostructures ranging from the microscale to the nanoscale, electrospinning has attracted extensive attentions in the past two decades [27–30]. RAMAKRISHNA et al [30] have reported direct fabrication of TiO_2 nanorods-graphene composite nanomaterials by electrospinning. The composite showed excellent photovoltaic and photocatalytic properties [31]. However, as far as we known, 1D graphene/TiO_2 composite with highly porous structure has not been prepared.

In this paper, the highly porous graphene/TiO_2 nanofibers were directly prepared by electrospinning. The composites displayed excellent photocatalytic performance for the degradation of Rhodamine B (RhB).

2 Experimental

The morphology of the graphene was investigated by scanning electron microscope (SEM, Hitachi S-4800) with an accelerating voltage of 5 kV and transmission electron microscope (TEM, FEI Tecnai F30) with an accelerating voltage of 300 kV. Figures 1(a)–(c) (SEM images) and Figure 1(d) (TEM image) present a typical 2D structure of graphene. Raman spectroscopy is used as an efficient way to identify graphene. Figure 1(e) shows Raman spectrum of our graphene sample by employing a LabRAM HR800 (HORIBA Jobin Yvon, France) confocal Raman spectrometer with an excitation laser wavelength of 600 nm. The major Raman features of graphene are so called G band (~1580 cm^{-1}) and 2D band (~2670 cm^{-1}). The G band originates from in-plane vibration of sp^2 carbon atoms and is a doubly degenerated (TO and LO) phonon mode (E_{2g} symmetry) at the Brillouin zone center. The 2D band originates from a two-phonon double resonance Raman process. Apparently, HRTEM can directly determine the number of graphene layers. The inset of Figure 1(e) HRTEM demonstrates few layers of graphene (about four layers).

2.1 Materials preparation

All the chemicals were of analytical grade and were used without further purification. The synthesis procedure of the graphene/TiO_2 composite nanofibers is presented in Figure 2. In the first step, 0.60 g tetrabutyl titanate was dissolved in 0.79 g ethanol and 1.05 g ethanoic acid (Tianjin Chemical Corp., China). This mixed solution was stirred for 20 min. Second, 0.2 g polyvinyl acetate (PVAC, Sigma Aldrich) was dissolved in N,N-dimethylformamide and stirred for 60 min. Then the two prepared solutions were mixed together and stirred for 1 h to obtain a viscous gel of PVAC/titanium acetate composite solution. At last, 0.2 g mineral oil (Tianjin Chemical Corp., China) and 4 mg graphene were added to the above solution and stirred at room temperature for 48 h to obtain a stable and homogeneous emulsion. The graphene was prepared by micromechanical cleavage in which highly oriented pyrolytic graphite was peeled by using a scotch tape [32, 33]. In a typical electrospinning process in our work, inner diameter of the spinneret was 0.6 mm. Grounded aluminum strips (1 cm in width) with parallel gaps about 1 cm were used as the collectors. The needle was connected to a high-voltage supply capable of generating DC voltage up to 60 kV. The voltage for electrospinning was kept at 18 kV. A distance of 15 cm was maintained between the tip of the spinneret and the collector. During the electrospinning process, the environmental temperature was maintained at 60 °C. After electrospinning, the fibers were heated from room temperature to 450 °C at a heating rate of 2 °C/min, and then held at 450 °C for 2 h in air.

2.2 Photocatalytic test

Absorption spectrum was tested by UV-Vis spectrum of powders using a TU-1901 spectrophotometer. The inset in Figure 2 shows a

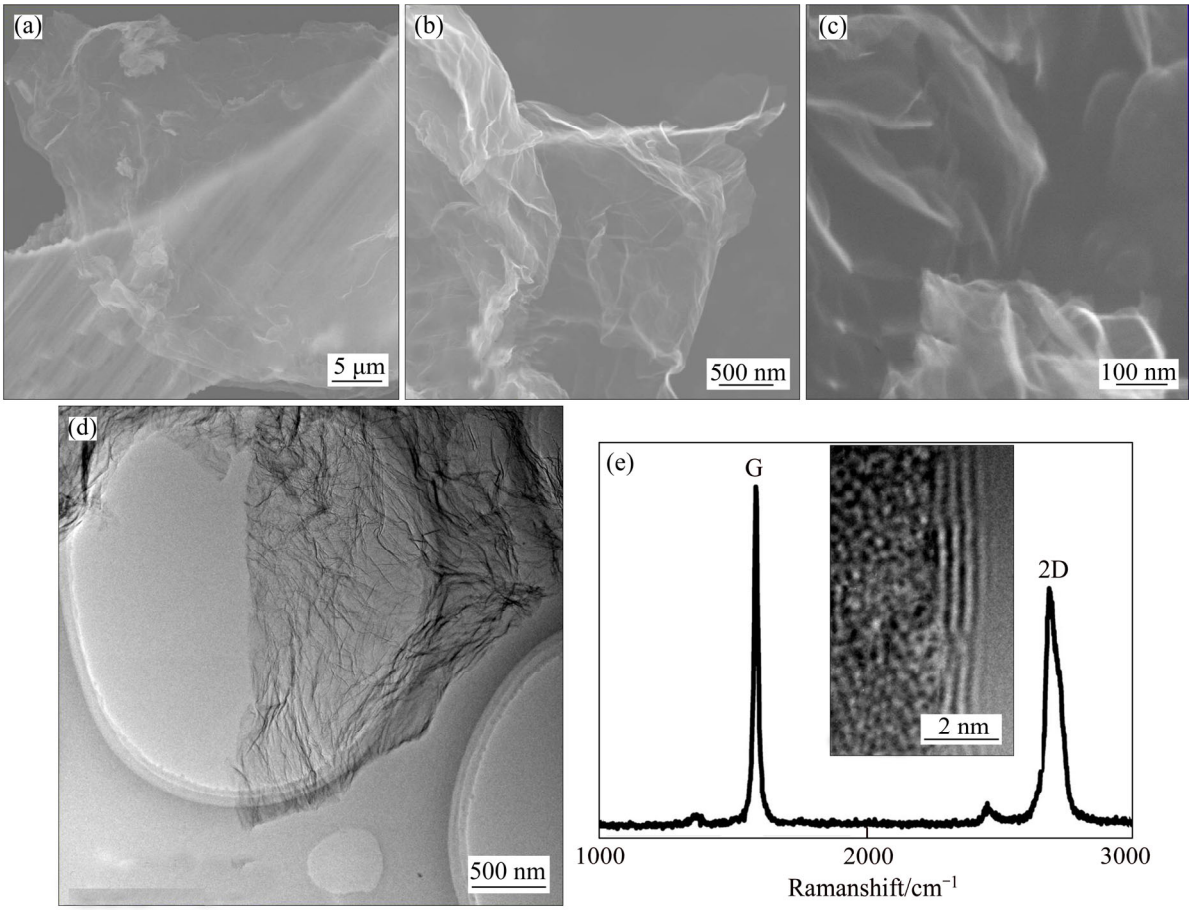

Figure 1 Scanning electron micrographs (a, b, c), transmission electron micrograph (d) of graphene and Raman spectrum of few layers of graphene (e) (the inset is high-resolution TEM (HRTEM) of graphene)

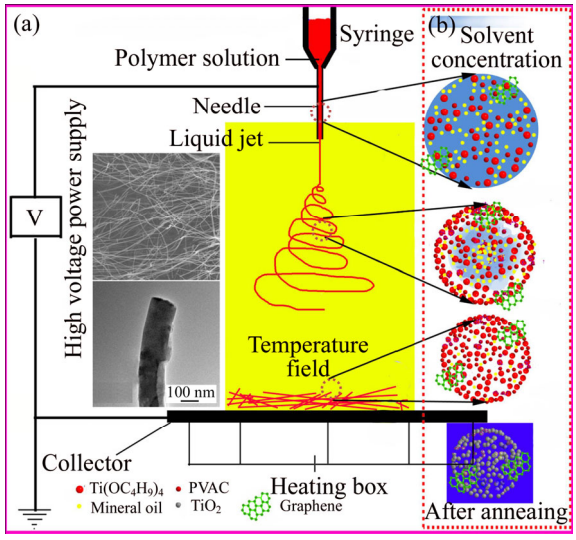

Figure 2 Schematic diagram of electrospinning fabrication of graphene and highly porous TiO_2 composite nanotubes (a) and proposed mechanism of formation of graphene and highly porous TiO_2 composite nanotubes (b)

possible mechanism of the formation of the graphene/TiO_2 composite nanofibers. During the electrospinning process (before the electrospun nanofibers were evenly distributed on the collector (Figure 2(a)), oil, ethanol and ethanoic acid began to evaporate once the fibers were spun out from the nozzle. The region of solvent evaporation near the surface of the fiber enriched in PVAC and tetrabutyl titanate (Figure 2(b)). The remaining solvent and oil evaporated from the fibers. Graphene–PVAC–tetrabutyl titanate nanofibers formed on the collector, and some oil remained in graphene–PVAC and tetrabutyl titanate. Because there was some oil in graphene–PVAC and tetrabutyl titanate, highly porous nanofibers can be achieved after annealing process [34].

3 Results and discussion

Figure 3(a) presents PVAC–tetrabutyl titanate nanofibers membrane containing graphene by electrospinning for 60 min. The inset in Figure 3(a)

is optical micrograph and clearly shows that well-aligned nanofibers are obtained by electrospinning over large area. Here, in order to get aligned nanofibers, a stainless steel U-shaped frame with a distance of 8 mm between two branches was used to transfer the aligned nanofibers by vertically moving through the gap. Our group demonstrated that the color of as-spun PVAC–tetrabutyl titanate nanofibers was usually white [9], which is an indirect proof of the homodisperse of graphene in PVAC–tetrabutyl titanate nanofibers. Figure 3(b) shows SEM image of the graphene/TiO_2 composite nanofibers, and the inset is the enlarged view of the nanofibers. Many pores with an average diameter of 15–20 nm are evenly distributed on the surface of the nanofibers, which can be further determined by TEM image. As shown in of Figure 3(c), the lattice spacing is measured to be 0.23 nm comparable to 0.25 nm for graphite. Additionally, the inset in Figure 3(a) displays a lattice spacing of 0.35 nm, corresponding to graphene (002). The lattice fringe of the area marked in Figure 3(d) is 0.35 nm, corresponding to (101) planes of anatase TiO_2. The selected area electron diffraction pattern of the nanofibers is shown in Figure 3(e) and demonstrates the composition of the graphene and TiO_2.

The photoactivities of as-synthesized samples were evaluated for photodecomposition of RhB under visible light irradiation. The RhB concentration (%) after various intervals of time could be estimated by using the following equation:

$$\text{RhB concentration} = \frac{A_t}{A_0} \times 100\%$$

where A_0 is the initial RhB absorbance at 554 nm (RhB shows a major absorption band at 554 nm) and A_t is the absorbance after various intervals of

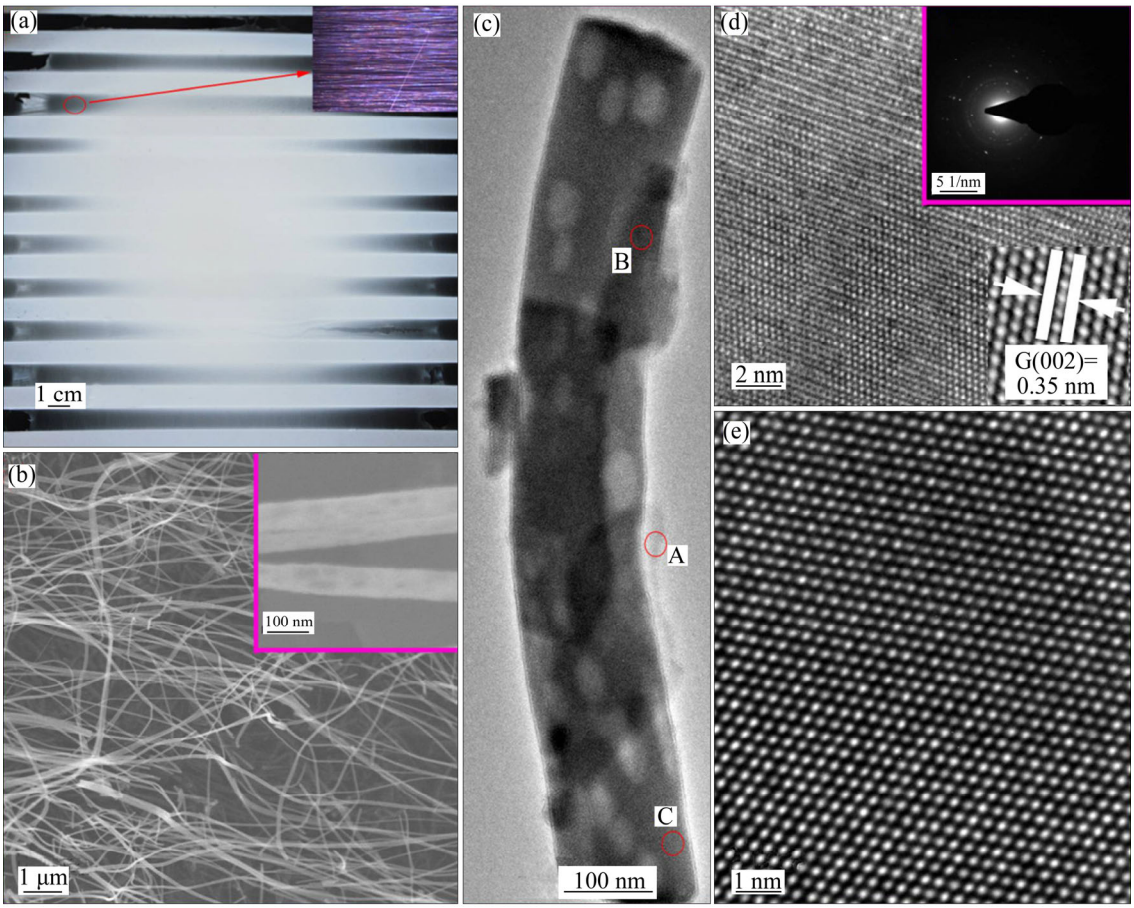

Figure 3 Photograph of PVAC/titanium acetate containing graphene nanosheets (a) (The inset is optical micrograph of the aligned nanofibers suspend over the U-shaped frame), scanning electron microscopy image of graphene and highly porous TiO_2 composite nanotubes (b) (The inset is enlarged image of the nanofibers), transmission electron microscopy image of graphene and highly porous TiO_2 composite nanotubes (c), High-magnification TEM (HRTEM) of region (d) (the insert show graphene interlayer spacing), and selected area electron diffraction pattern (e) of HRTEM lattice image taken from graphene and highly porous TiO_2 composite nanotubes marked by C

time *t*. To eliminate the effect of heating during irradiation, the beaker was immersed in an ice–water mixture. To demonstrate the excellent photocatalytic performance of highly porous graphene/TiO_2 composite-nanofibers, TiO_2 nanofibers were synthesized for comparisons. The evolution of the corresponding UV–Vis spectrum with UV exposure time is presented in Figure 4(a). It can be observed that the graphene/TiO_2 nanofibers composite presents more prominent photocatalytic activity. After 120 min irradiation, almost 100 % of the RhB molecules were decomposed by the porous graphene/TiO_2 nanofibers composite, while about 25% RhB molecules were intacted by the TiO_2 nanofibers as the photocatalyst. The ratio of RhB molecules self-decomposed is also shown for comparison in Figure 4(a). Moreover, the graphene/TiO_2 nanofibers composite exhibits very stable photocatalytic activity. There is no obvious decrease in the removal rate of RhB even after 10 cycles as shown in Figure 4(b). This phenomenon may be attributed to the photocatalytic process that the catalyst change is physical change, while the structure of the catalyst is not influenced.

Absorption range is very important in the photocatalysis [35], especially for the visible light photo degradation of contaminants. There is an obvious red shift of 20–30 nm in the absorption edge of highly porous graphene/TiO_2 nanofibers composite compared to pure TiO_2 nanofibers. This red shift should be attributed to the follow reasons: 1) TiO_2 and graphene can form Ti—O—C bond, similar to the case of carbon doped TiO_2 composites [36]; 2) Owing to the coupling of a small band gap or band gap-less semiconductor material of graphene with TiO_2, the visible light absorption capability of highly porous graphene/TiO_2 nanofibers composite is greatly enhanced as compared with TiO_2 nanofibers (Graphene was found to absorb a significant fraction of incident white light) [37, 38]. Therefore, a more efficient utilization of the solar spectrum could be achieved due to the extended photo responding range of 420–430 nm.

As also shown in Figure 5, there is an obvious red shift ranging from 10 to 25 nm in the absorption edge of the highly porous graphene/TiO_2 nanofibers composite, which may be attributed to

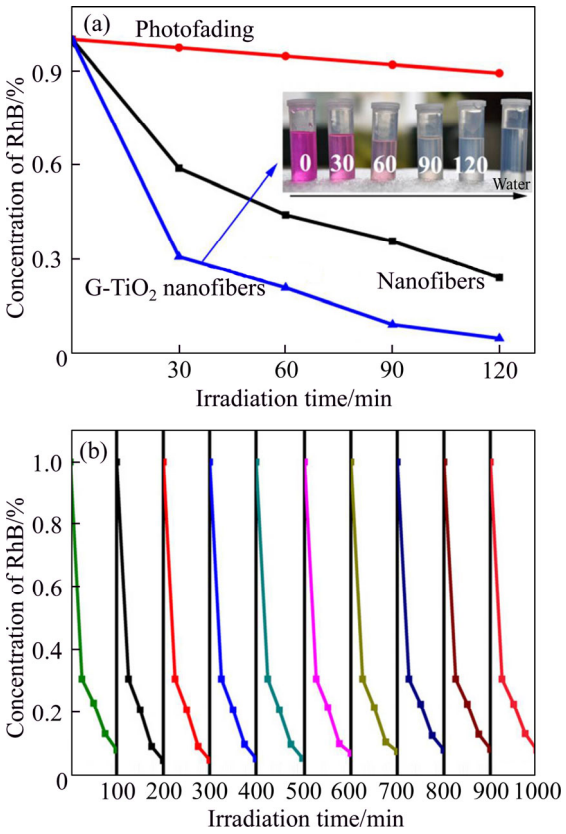

Figure 4 Photograph of Rhodamine B carried out under visible light irradiation for different time (a) and cycling tests of photocatalytic activity of graphene composite highly porous/TiO_2 nanofibers (b) (Catalyst 60 mg; 10 mg/L RhB 50 mL; 250 W mercury lamp; Luminous range 380–800 nm)

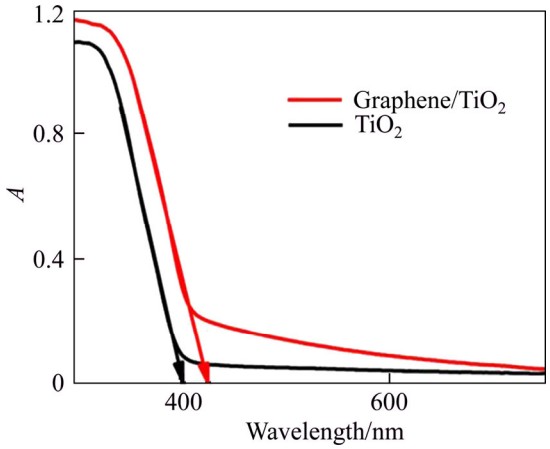

Figure 5 Absorption spectrum of graphene/highly porous TiO_2 nanofibers composite and pure TiO_2 nanofibers

the graphene with zero band gap introducing to TiO_2 nanofibers compared to pure TiO_2 nanofibers. The photoactivity of the highly porous graphene/TiO_2 nanofibers catalyst is expected to

facilitate its use in practical environmental remediation.

The photocatalyst stability has further been confirmed by XRD (before and after cycle test) in Figure 6(a). The XRD peaks unchanged after cycle test compared with XRD before cycle test, indicating that the photocatalyst is stable [39]. The photocatalytic degradation mechanism of RhB is proposed in Figure 6(b). Under UV-visible light irradiation, TiO_2 is excited. Some electrons can be quickly injected into the graphene from the CB of TiO_2•. The separated electrons can directly react with the dissolved oxygen molecules for yielding superoxide radical anions (O_2•$^-$), then the superoxide radical anions experience protonation to generate hydroperoxy (HO_2•), and the HO_2• can further react with H_2O to produce •OH [40, 41]. Meanwhile, the h^+ can directly react with RhB and also react with H_2O to produce •OH. Finally, RhB can be decomposed by the generated radicals and holes.

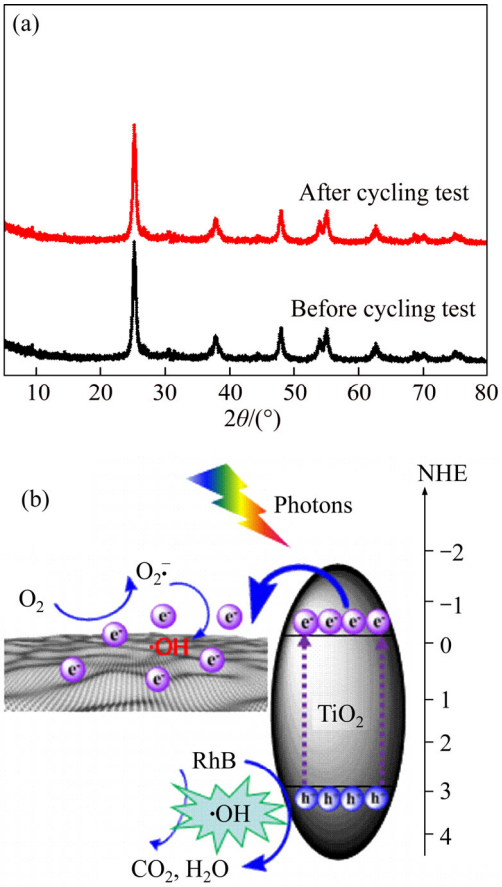

Figure 6 XRD patterns of graphene/TiO_2 composite before and after cycle test (a) and diagram of photocatalytic reaction of RhB on graphene/TiO_2 composite (b)

4 Conclusions

Graphene/TiO_2 nanofibers composite was directly fabricated by electrospinning. The graphene can uniformly disperse in the highly porous TiO_2 nanofibers. The highly porous graphene/TiO_2 nanofibers composite displayed excellent photocatalytic performance for the degradation of RhB. Such highly porous graphene/TiO_2 nanofibers composite may bring new insights into the design of highly efficient photo catalysts for organic compounds and may have potential technological applications. This new method is anticipated to open a new possibility in the investigation of graphene/TiO_2 composites and other metal oxide/graphene composite and promote their application in lithium ion batteries, hydrogen preparation, and so on.

References

[1] CUI Yi, WEI Qing-qiao, PARK H, LIEBER C. Nanowire nanosensors for highly sensitive and selective detection of biological and chemical species [J]. Science, 2001, 293: 1289–1292.

[2] LU Bing-an, WANG Ya-jiang, LIU Yan-xia, DUAN Hui-gao, ZHOU Jin-yuan, ZHANG Zhen-xing, WANG You-qing, LI Xiao-dong, WANG Wei, LAN Wei, XIE Er-qing. Superhigh-throughput needleless electrospinning using a rotary cone as spinneret [J]. Small, 2010, 6: 1612–1616.

[3] LU Bing-an, ZHANG Zhen-xing, BAO Zhong, LI Xiao-dong, LIU Yan-xia, ZHU Chen-quan, DUAN Hui-gao, XIE Yi-zhu, WANG You-qing, XIE Er-qing. Carbon nanonodules fewer than ten graphenes thick grown on aligned amorphous carbon nanofibers [J]. Carbon, 2011, 49: 1939–1945.

[4] ZHU Jian, ZHANG Guan-hua, YU Xin-zhi, LI Qiu-hong, LU Bing-an. Graphene double protection strategy to improve the SnO_2 electrode performance anodes for lithium-ion batteries [J]. Nano Energy, 2014, 3: 80–87.

[5] DUAN Hui-gao, XIE Er-qing, HAN Li, XU Zhi. Turning PMMA nanofibers into graphene nanoribbons by in situ electron beam irradiation [J]. Advanced Materials, 2008, 20: 3284–3288.

[6] ZHU Jian, XU Zhi, LU Bing-an. Ultrafine Au nanoparticles decorated $NiCo_2O_4$ nanotubes as anode material for high-performance supercapacitor and lithium-ion battery applications [J]. Nano Energy, 2014, 7: 114–123.

[7] WANG Long-lu, LI Yue, LIU Yu-tang. Reduced graphene oxide@ TiO_2 nanorod@ reduced graphene oxide hybrid nanostructures for photoelectrochemical hydrogen production [J]. Micro & Nano Letters, 2017, 12(7): 494–496.

[8] GIRIT C, MEYER J, ERNI R, ROSSELL M, KISIELOWSKI C, YANG Li, PARK C, CROMMIE M, COHEN M, LOUIE S, ZETTL A. Graphene at the edge:

Stability and dynamics [J]. Science, 2009, 323: 1705–1708.
[9] LU Bing-an, LI Ting, ZHAO Hai-tao, LI Xiao-dong, GAO Cai-tian, ZHANG Sheng-xiang, XIE Er-qing. Graphene-based composite materials beneficial to wound healing [J]. Nanoscale, 2012, 4: 2978–2982.
[10] HU Wen-bing, PENG Cheng, LUO Wei-jie, LU Min, LI Xiao-ming, LI Di, HUANG Qing, FAN Chun-hai. Graphene-based antibacterial paper [J]. ACS Nano, 2010, 4: 4317–4323.
[11] STANDLEY B, BAO Wen-zhong, ZHANG Hang, BRUCH J, LAU Chun-ning, BOCKRATH M. Graphene-based atomic-scale switches [J]. Nano Letter, 2008, 8: 3345–3349.
[12] STANKOVICH S, DIKIN D, DOMMETT G, KOHLHAAS K, ZIMNEY E, STACH E, PINER R, NGUYEN S, RUOFF R. Graphene-based composite materials [J]. Nature, 2006, 442: 282–286.
[13] STOLLER M, PARK S, ZHU Y, AN J, RUOFF R. Graphene-based ultracapacitors [J]. Nano Letter, 2008, 8(10): 3498–3502.
[14] ALLEN M, TUNG V, KANER R. Honeycomb carbon: A review of graphene [J]. Chemical Reviews, 2009, 110: 132–145.
[15] ZHANG Yin, NAYAK T, HONG H, CAI Wei-bo. Graphene: A versatile nanoplatform for biomedical applications [J]. Nanoscale, 2012, 4: 3833–3842.
[16] LI Xiao-dong, ZHANG Yong-zhe, ZHANG Zhen-xing, ZHOU Jing-yuan, SONG Jie, LU Bing-an, XIE Er-qing, LAN Wei. Electrospraying tuned photoanode structures for dye-sensitized solar cells with enhanced energy conversion efficiency [J]. Journal of Power Sources, 2011, 196: 1639–1644.
[17] WANG Bo, CHEN Zhi-ming, ZHANG Jia-nan, CAO Jing-jing, WANG Shu-xia, TIAN Qiu-ge, GAO Ming, XU Qun. Fabrication of PVA/graphene oxide/TiO_2 composite nanofibers through electrospinning and interface sol-gel reaction: Effect of graphene oxide on PVA nanofibers and growth of TiO_2 [J]. Colloids and Surfaces A: Physicochemical and Engineering Aspects, 2014, 457: 318–325.
[18] PANT H, ADHIKARI S, PANT B, JOSHI M, KIM H, PARK C, KIM C. Immobilization of TiO_2 nanofibers on reduced graphene sheets: Novel strategy in electrospinning [J]. Journal of Colloid and Interface Science, 2015, 457: 174–179.
[19] KIM C, KIM B, YANG K. TiO_2 nanoparticles loaded on graphene/carbon composite nanofibers by electrospinning for increased photocatalysis [J]. Carbon, 2012, 50: 2472–2481.
[20] ZHAO Yin, LI Chun-zhong, LIU Xiu-hong, GU Feng. Highly enhanced degradation of dye with well-dispersed TiO_2 nanoparticles under visible irradiation [J]. Journal of Alloys and Compounds, 2007, 440: 281–286.
[21] ZHENG S, WANG T, HAO W, SHEN R. Improvement of photocatalytic activity of TiO_2 thin film by Sn ion implantation [J]. Vacuum, 2002, 65: 155–159.
[22] ZHANG Hao, LV Xiao-jun, LI Yue-ming, WANG Ying, LI Jing-hong. P25-graphene composite as a high performance photocatalyst [J]. ACS Nano, 2009, 4: 380–386.
[23] CHEN Jun-song, WANG Zhi-yu, DONG Xiao-chen, CHEN Peng, LOU Xiong-wen. Graphene-wrapped TiO_2 hollow structures with enhanced lithium storage capabilities [J]. Nanoscale, 2011, 3: 2158–2161.
[24] DING Shu-jiang, CHEN Jun-song, LUAN De-yan, BOEY F, MADHAVI S, LOU Xiong-wen. Graphene-supported anatase TiO_2 nanosheets for fast lithium storage [J]. Chemical Communications, 2008, 8: 5780–5782.
[25] FENG Xin-jian, SHANKAR K, VARGHESE O, PAULOSE M, LATEMPA T, GROMES C. Vertically aligned single crystal TiO_2 nanowire arrays grown directly on transparent conducting oxide coated glass: synthesis details and applications [J]. Nano Letter, 2008, 8: 3781–3786.
[26] ZHU Kai, NEALE N, MIEDANER A, FRANK A. Enhanced charge-collection efficiencies and light scattering in dye-sensitized solar cells using oriented TiO_2 nanotubes arrays [J]. Nano Letter, 2007, 7: 69–74.
[27] LI Dan, WANG Yu-liang, XIA You-nan. Electrospinning nanofibers as uniaxially aligned arrays and layer-by-layer stacked films [J]. Advanced Materials, 2004, 16: 361–366.
[28] LI Dan, XIA You-nan. Electrospinning of nanofibers: reinventing the wheel? [J]. Advanced Materials, 2004, 16: 1151–1170.
[29] LU Xiao-feng, WANG Ce, WEI Yen. One-dimensional composite nanomaterials: Synthesis by electrospinning and their applications [J]. Small, 2009, 5: 2349–2370.
[30] RAMAKRISHNA S, FUJIHARA K, TEO W, YONG T, MA Zu-wei, RAMASESHAN R. Electrospun nanofibers: Solving global issues [J]. Materials Today, 2006, 9: 40–50.
[31] ZHU Pei-ning, NAIR A, PENG Sheng-jie, YAN Sheng-yuan, RAMAKRISHNA S. Facile fabrication of TiO_2-graphene composite with enhanced photovoltaic and photocatalytic properties by electrospinning [J]. ACS Applied Materials & Interfaces, 2012, 4: 581–585.
[32] ZHU Jian, LEI Dan-ni, ZHANG Guan-hua, LU Bing-an, WANG Tai-hong. Carbon and graphene double protection strategy to improve the SnO_x electrode performance anodes for lithium-ion batteries [J]. Nanoscale, 2013, 5: 5499–5505.
[33] ZHU Jian, ZHANG Guan-hua, YU Xin-zhi, LI Qiu-hong, LU Bing-an, XU Zhi. Graphene double protection strategy to improve the SnO_2 electrode performance anodes for lithium-ion batteries [J]. Nano Energy, 2014, 3: 80–87.
[34] LU Bing-an, ZHU Cheng-quan, ZHANG Zhen-xing, LAN Wei, XIE Er-qing. Preparation of highly porous TiO_2 nanotubes and their catalytic applications [J]. Journal of Materials Chemistry, 2012, 22: 1375–1379.
[35] LINSEBIGLER A, LU Guang-quan, YATES Y. Photocatalysis on TiO_2 surfaces: Principles, mechanisms, and selected results [J]. Chemical Reviews, 1995, 95: 735–758.
[36] INAGAKI M, KOJIN F, TRYBA B, TOYODA M. Carbon-coated anatase: The role of the carbon layer for photocatalytic performance [J]. Carbon, 2005, 43: 1652–1659.
[37] NAIR R, BLAKE P, GRIGORENKO A, NOVOSELOV K, BOOTH T, STAUBER T, PERES N, GEIM A. Fine structure constant defines visual transparency of graphene [J]. Science, 2008, 320: 1308–1309.
[38] ABERGEL D, FALO V. Optical and magneto-optical far-infrared properties of bilayer graphene [J]. Physical Review B, 2007, 75: 155430.
[39] TANG D, ZHANG G. Fabrication of $AgFeO_2$/g-C_3N_4

nanocatalyst with enhanced and stable photocatalytic performance [J]. Applied Surface Science, 2017, 391: 415–422.

[40] TANG D, ZHANG G. Ultrasonic-assistant fabrication of cocoon-like Ag/$AgFeO_2$ nanocatalyst with excellent plasmon enhanced visible-light photocatalytic activity [J]. Ultrasonics Sonochemistry, 2017, 37: 208–215.

[41] WAN Z, ZHANG G, WU X, YIN S. Novel visible-light-driven Z-scheme $Bi_{12}GeO_{20}$/g-C_3N_4 photocatalyst: Oxygen-induced pathway of organic pollutants degradation and proton assisted electron transfer mechanism of Cr(VI) reduction [J]. Applied Catalysis B: Environmental, 2017, 207: 17–26.

(Edited by YANG Hua)

中文导读

静电纺丝制备高度多孔石墨烯/TiO_2复合材料的纳米纤维及光催化性能研究

摘要：本文报道了一种利用静电纺丝制备高度多孔的石墨烯/TiO_2 复合材料纳米纤维的方法。该方法通过静电纺丝将石墨烯与有机钛源复合，经 450 °C 焙烧后得到分布均匀、具有高度多孔的石墨烯/TiO_2 复合材料纳米纤维。该复合材料表现出优异的光催化性能。制备石墨烯/TiO_2 复合材料纳米纤维的新方法用途广泛，可用于制备各种金属氧化物和石墨烯纳米复合材料。

关键词：多孔结构；石墨烯；二氧化钛；光催化应用